Sakarya University Journal of Science
SAUJS

Title: Thermal Effect Estimation of Smartphone Virtual Reality Headsets on Human Eye by Finite Element Method

Authors: Niyazi ULUAYDIN, Selim ŞEKER

Thermal Effect Estimation of Smartphone Virtual Reality Headsets on Human Eye by Finite Element Method

Niyazi ULUAYDIN*[1], Selim ŞEKER[2]

Abstract

Smartphones (SP) terminals are becoming the most popular media for virtual reality (VR) and augmented reality (AR) effects with their central processing unit (CPU) and video capabilities. Simple VR headsets with reasonable costs can host smartphones, and they can together be used for many different applications. But with the outbreak of Covid-19 pandemic, their usage has become essential for many people working from their homes. VR and AR capabilities provide a much richer experience for entertainment, gaming, and video conferencing. The increasing popularity of 3D virtual worlds add up to this usage. On the technology side, multi-radio connectivity is supported both on terminal and network side. A certain risk may arise when using SP VR headsets for such applications requiring a broadband Internet connectivity. SPs with multi-radio connectivity feature may elevate specific absorption rate (SAR) values in those cases. The smartphone used for VR and AR applications is positioned in front of the eyes; and there is very limited ventilation in VR/AR headsets. Authors' model aims simulate these exposure scenarios in 4G and 5G mobile telecommunication frequencies by finite element method (FEM); and, possible thermal and non-thermal risks of related electromagnetic (EM) radiation on human eye according to the outputs of the model are discussed.

Keywords: Electromagnetic radiation effects, SAR, smartphone, Virtual Reality headset, Thermal effects on human eye, 5G.

1. INTRODUCTION

The SP terminals and the mobile telecommunication technologies both have great developments in recent years. The number of mobile users has passed beyond 5 billion as of 2022 [1]. On the terminal side, SPs are now equipped with more powerful processors and with much higher resolution displays. Similarly, the new generation mobile telecommunication

* Corresponding author: korkut@uluaydin.com
[1] Boğaziçi University
ORCID: https://orcid.org/ 0000-0002-9512-0077
E-mail: selim.seker@uskudar.edu.tr
[2] Üsküdar University/Faculty of Engineering and Natural Sciences/Department of Electrical-Electronics Engineering
ORCID: https://orcid.org/ 0000-0002-0980-3219

Niyazi ULUAYDIN, Selim ŞEKER

Thermal Effect Estimation of Smartphone Virtual Reality Headsets on Human Eye by Finite Element Metho...

technologies can now support broadband Internet connectivity with much lower latencies. In order to sustain the broadband access in dense urban area, the mobile telecommunication industry supports mobile broadband Internet connectivity by the fixed line broadband Internet access through a secondary wireless local area network (WLAN/Wi-Fi) technology. For this reason, almost all new SP terminals support two simultaneously working radio units.

The SP AR/VR headset users have dramatically increased during the corona virus disease 2019 (COVID-19) pandemic for social distancing reasons and is expected to pass beyond 1 billion users in 2022 [2,3]. In the case of a SP VR headset usage, the application would generally require broadband Internet access. In new classes of SP terminals, which are supporting two simultaneous radio accesses such as Wi-Fi and Long Term Evolution (LTE/4G or 5G or beyond) concurrently, high data throughputs can be achieved [. The SP VR headset hosts the SP terminal right before the eyes. The headsets are made of lightweight materials, and these materials have little or no electromagnetic (EM) shielding properties. Therefore, there will be EM radiation exposure from a very short distance at a right angle. Secondly, most of the SP VR headsets fully limit the natural air flow to block the ambient light from surroundings for a better visual experience. Since the subject human will supposedly have a visual experience on a SP VR headset for a certain period, the wireless connectivity will be on for the same period. This kind of usage can build up higher than normal thermal heating from EM radiation.

In this study, the authors are going to simulate these thermal effects on human eye by finite element method (FEM). This EM effect can be detrimental especially on eyes, since human eye cools itself by corneal evaporation and retinal blood perfusion [4,5]. Lacking any of those would increase the temperatures to levels that could pose immediate risks. One may presume retinal blood perfusion unchanged, whereas SP headset surely limits the natural cooling of the eyes with ambient air. Our literature survey has not come across with any studies on the subject.

The rest of the paper is organized as follows: Section 2 describes employed simulation model and methodology; Section 3 presents simulation results; Section 4 provides the brief discussion of the simulation results, and finally Section 5 discusses experimental findings and its possible thermal and non-thermal effects on human eye.

2. SIMULATION MODEL AND METHODOLOGY

2.1. Simulation Model

We have used the IEEE head phantom model for Specific Absorption Rate (SAR) calculation in the simulation software Comsol Multiphysics (MP) 4.3 (FNL License No: 17073372) [5]. Comsol MP is based on finite element method (FEM). FEM approach has a high computational complexity, but it defines objects with curvature better than the finite difference time domain method (FTDT) [5,7]. For the eye part, we have used the realistic three-dimensional (3D) eye model by Bobby Dyer from the web [8]. We have simplified this eye model as if eye tissue is either sclera or vitreous humour to decrease the immense computational load. And finally, this eye model is embedded as a separate domain into the IEEE head phantom model in our simulation software (Figure 1) [6-8].
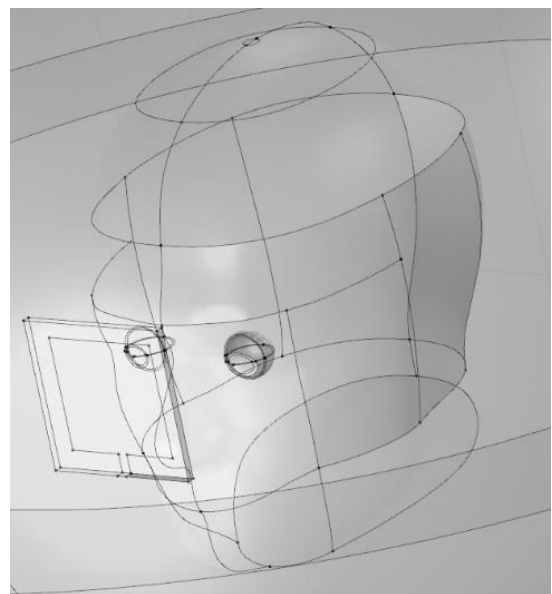
Figure 1 IEEE head phantom model with eyes.

Niyazi ULUAYDIN, Selim ŞEKER

Thermal Effect Estimation of Smartphone Virtual Reality Headsets on Human Eye by Finite Element Metho...
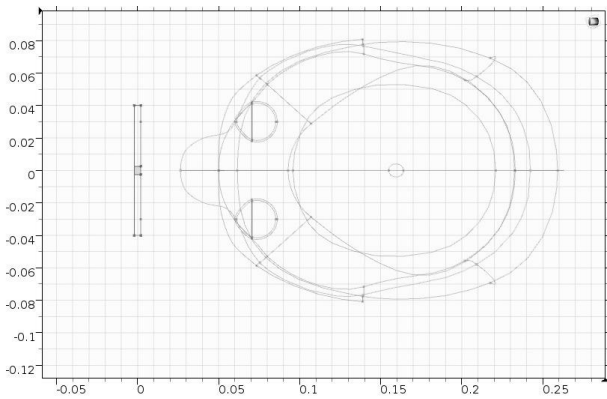
Figure 2 Top-down view of central antenna position at 5cm according to IEEE head phantom model with eyes (all values in meter).

Two uniform lump ports are used to resemble the SP EM sources with nominal output powers as in the original model SAR setting with equal powers of 1.6 W to match the smartphone SAR limit [9]. One of the EM sources is fixed at Wi-Fi frequency on 2.45 GHz, and the other EM source is parametric at mobile telecommunication frequency bands of 4G and 5G at 800, 900, 1800, 2100, 2300, and 2600 MHz. We have assumed both antennas to be in the same position in the central axis of eyes vertically and in central plane of eye, horizontally (Figure.2). On the side antenna scenario, both antennas are horizontally shifted 0.03 m from the central axis to align with one of the eyes. The distance from antenna to the phantom model is also parametric to investigate the effects of EM propagation and heating in the eye from different SP VR headsets.

The SAR model solves the vector Helmholtz equations in the head and eye domains for each of the frequencies and transfers the SAR solution onto the Pennes' bioheat equation to calculate the corresponding temperature rise in related domains [7].

2.2. Simulation Parameters and Settings

Our IEEE phantom model uses the 3D magnetic resonance imaging-based tissue separation [10] to use appropriate blood perfusion, conductivity, and permittivity properties for brain [11, 12]. We take the retinal blood perfusion rate to be the same with brain (Table.1).

Table 1 Human Head Tissue Blood Perfusion Rates.

Part	Perfusion Rate
Brain	$2 \cdot 10\text{-}3$ (ml/s)/ml
Bone	$3 \cdot 10\text{-}4$ (ml/s)/ml
Skin	$3 \cdot 10\text{-}4$ (ml/s)/ml

Table 2 Tissue Conductivity Values [S/m].

Frequency (MHz)	Sclera	Vitreous Humour	Brain
800	1.130272	1.608266	0.730524
900	1.166726	1.636162	0.766504
1800	1.601727	2.032478	1.15308
2100	1.789117	2.221833	1.310172
2300	1.925249	2.363649	1.422798
2450	2.033048	2.478094	1.511336
2600	2.145607	2.599401	1.603296

Table 3 Tissue Relative Permittivity Values

Frequency (MHz)	Sclera	Vitreous Humour	Brain
800	55.561417	68.925781	46.251328
900	55.27013	68.90184	45.805496
1800	53.567787	68.573364	43.544899
2100	53.125057	68.417976	43.054611
2300	52.839252	68.301758	42.754364
2450	52.627628	68.208023	42.538925
2600	52.417377	68.108711	42.329929

We have modelled the eye as a single tissue. Thus, we have used two sets of conductivity (σ) and relative permittivity (ε$_r$) to understand the effects representing the eye as if it is sclera only (lower water content) or vitreous humour only (higher water content) (Table 2-3). In the simulations, all frequency dependent values are piecewise linearly interpolated between 800 and 2600 MHz values.

As mentioned before, the SP VR headsets limit the airflow inside. The SP also produces heat towards the face by its display. In our samplings, we have found out that the SP VR headset inner volume was equal or less than 0.0015 m^3. During its operation, the air inside the SP VR headset will have high vapor pressure in a short time with corneal and epidermal evaporation. Naturally, further evaporation from the cornea surface will be limited. For these reasons, we have taken the eye-air boundary as thermal insulation. Finally,

Niyazi ULUAYDIN, Selim ŞEKER

Thermal Effect Estimation of Smartphone Virtual Reality Headsets on Human Eye by Finite Element Metho...

we have totally neglected eye movement in VR usage.

We set the simulation environment to be under standard pressure at 25°C, and the temperature scale is normalized to 0 to represent the fluctuation from the nominal biological base temperature of 37°C. The heat capacity of blood is taken as 3639 J/(kg·K) and the density of blood is taken as 1000 kg/m³.

There has been extensive academic research on human eye temperature distribution [4, 5, 13-15]. Infrared detection, which is the most recent and non-invasive empirical technique, has shown that the cornea surface temperature for human eye can be referred as 34.3°C [5]. Similarly, the retinal blood temperature can be referred as 37°C [5, 13]. We have set the initial conditions of the simulation respective to these figures, which have a great effect on the outcome for different domains.

The simulations used one frequency of the radio units fixed at 2450 MHz representing the wireless connection, whereas the other radio unit frequency spanned the frequencies of 800, 900, 1800, 2100, 2300, and 2600 MHz, representing the mobile network connection. Eye tissue has been simulated as either it is made of all sclera or vitreous humour. The distance is calculated by the gap between the antennas and the forehead in the model. There is an additional 1 cm depth difference between the forehead and the eye. Having sampled different SP VR headsets, we have decided to make different simulations at 4 different distance values as 2, 3, 5, and 7 cm, which were dominant in our VR gap sampling.

3. SIMULATION OUTCOMES AND THEIR DISCUSSIONS

3.1. Simulation Outcomes

We have made the simulation over 4 different distances running over a 60- minute exposure to detect distance effects and possible saturation times. The general saturation values were around

15th minute. For lower frequencies with higher tissue penetration the retinal part of the eye could build up more heat until the 20th minute. For higher frequencies, the saturation happened around the 12th minute mark. The highest rise in temperature was observed at 5 cm for central antenna position and at 3 cm for side antenna position. Finally, the tissue type also affects the temperature rise.

In figures 3, 4, and 5, one can observe the temperature increase from concurrent 2450 MHz and 2600 MHz EM sources. Figure 5 shows the whole model, whereas figures 3 and 4 show the eye domain isolated from the rest of the phantom to visualize the temperature distribution in detail.
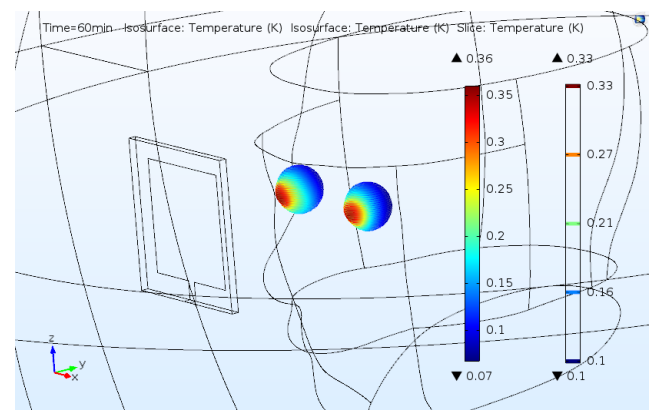
Figure 3 Isosurface temperature rise plot in human eye as vitreous humour tissue only exposed to 2450 MHz-2600 MHz with central antennas at 5 cm.
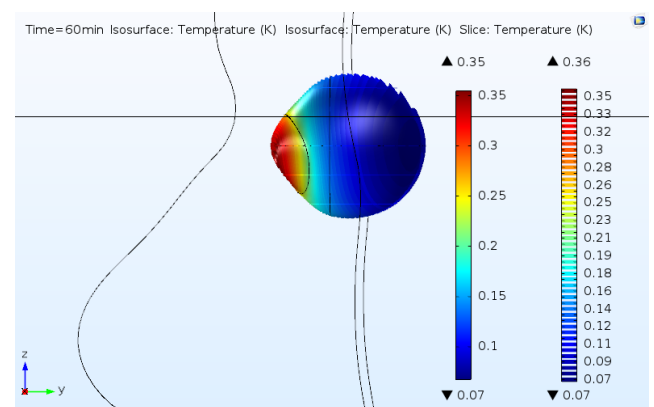
Figure 4 Side-view 25 slice isosurface temperature rise plot in human eye as vitreous humour tissue only exposed to 2450 MHz-2600 MHz with central antennas at 5 cm.
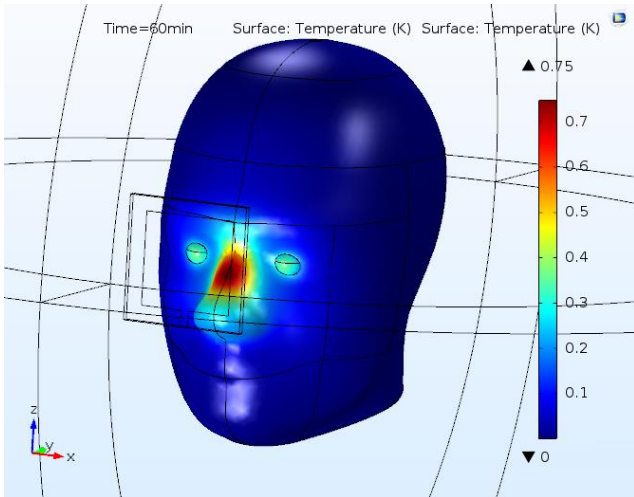
Figure 5 Surface temperature rise plot in human eye as vitreous humour tissue only exposed 2450 MHz-2600 MHz with central antennas at 5 cm.

In tables 4 and 5, one can observe the corneal and retinal temperature increase at 5 cm distance between the face and the SP terminal. The highest temperature increase happens at 5 cm with vitreous humour tissue only eye domain with 0.07 ^{o}C (Table 5).

Table 4 Simulation results at 5 cm with central antennas (eye tissue-sclera).

Frequency (MHz)	Corneal Temp.	Retinal Temp.
800-2450	0.12 ^{o}C	0.03 ^{o}C
900-2450	0.14 ^{o}C	0.03 ^{o}C
1800-2450	0.16 ^{o}C	0.03 ^{o}C
2100-2450	0.23 ^{o}C	0.05 ^{o}C
2300-2450	0.20 ^{o}C	0.05 ^{o}C
2450-2600	0.34 ^{o}C	0.06 ^{o}C

Table 5 Simulation results at 5 cm with central antennas (eye tissue-vitreous humour).

Frequency (MHz)	Corneal Temp.	Retinal Temp.
800-2450	0.14 ^{o}C	0.03 ^{o}C
900-2450	0.16 ^{o}C	0.03 ^{o}C
1800-2450	0.17 ^{o}C	0.03 ^{o}C
2100-2450	0.25 ^{o}C	0.05 ^{o}C
2300-2450	0.21 ^{o}C	0.05 ^{o}C
2450-2600	0.35 ^{o}C	0.07 ^{o}C

3.2. Simulation Outcomes' Discussions

The simulations have shown interesting results. The corneal temperature increase has reached 0.35^{o}C at a distance of 5 cm from face with 2450-2600 MHz pair in central antennas scenario (Figure 6). In the side antennas scenario, the corneal temperature increase has further reached 0.7^{o}C at a distance of 3 cm from face with 2450-2600 MHz pair (Figure 7). It is important remember that natural cornea temperature is 34.3^{o}C and the initial conditions are set accordingly as 2.7^{o}C below nominal body temperature of 37 ^{o}C. So, there is a total increase of 3.05^{o}C with central antennas and 3.41^{o}C with side antennas, respectively. To assess this risk, one should consider other factors as blinking rate and evaporation rate.
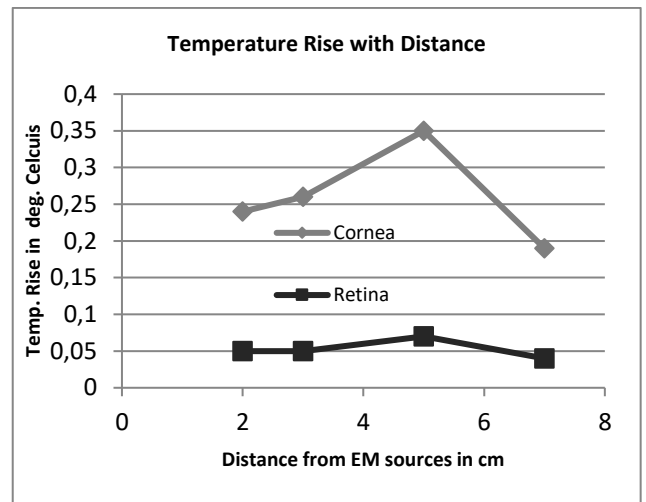
Figure 6 Temperature rise plot in human eye as vitreous humour tissue only exposed to 2450 MHz-2600 MHz central antennas at varying distances.
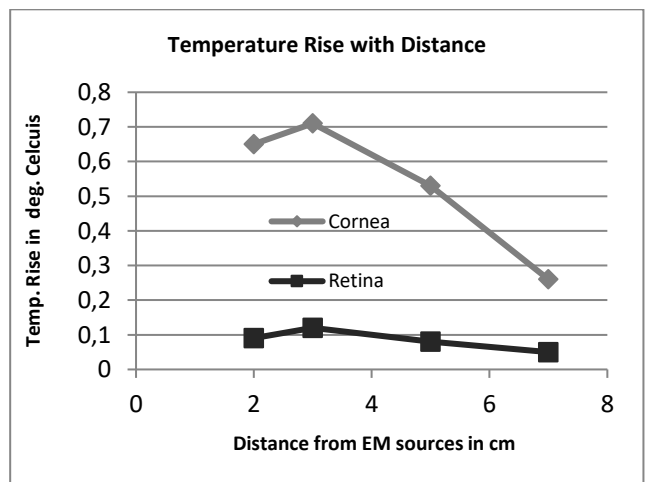
Figure 7 Temperature rise plot in human eye as vitreous humour tissue only exposed to 2450 MHz-2600 MHz side antennas at varying distances.

Niyazi ULUAYDIN, Selim ŞEKER

Thermal Effect Estimation of Smartphone Virtual Reality Headsets on Human Eye by Finite Element Metho...
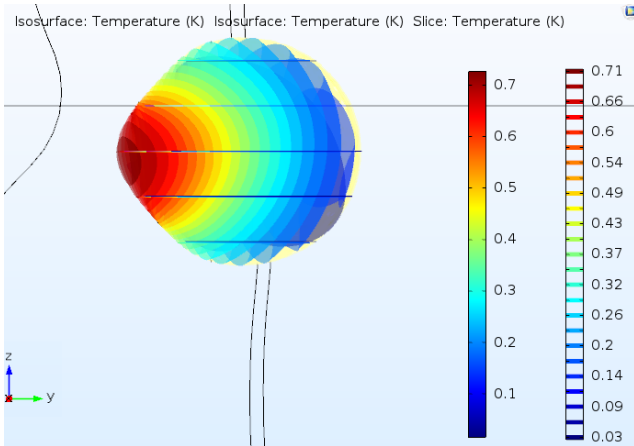
Figure 8 Side-view 25 slice isosurface temperature rise plot in human eye as vitreous humour tissue only exposed to 2450 MHz-2600 MHz with side antennas at 3 cm.
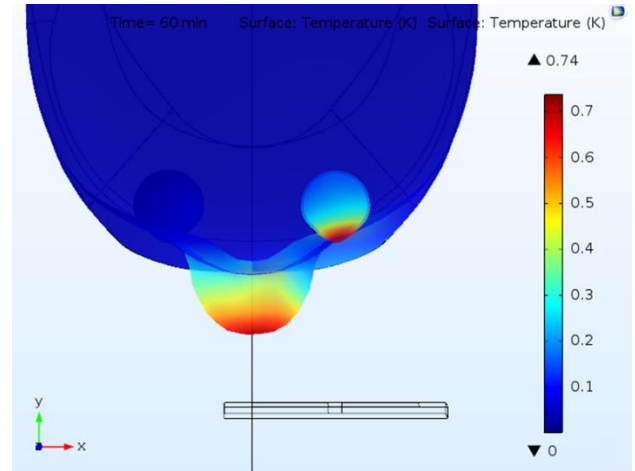
Figure 10 Transparent top-down view temperature rise plot in human eye as vitreous humour tissue only exposed to 2450 MHz-2600 MHz with side antennas at 3 cm.
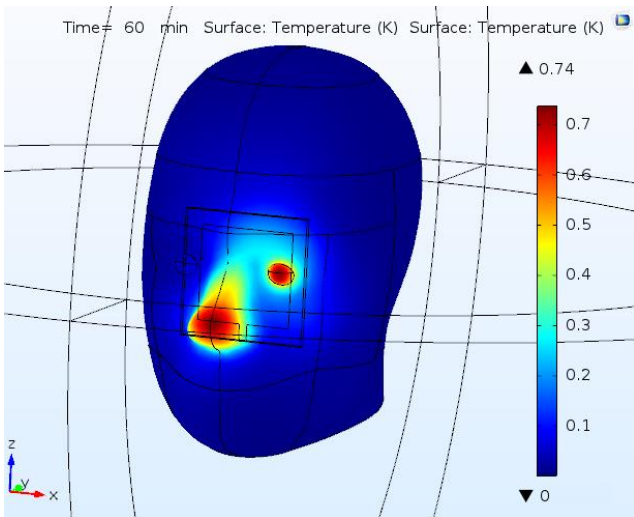
Figure 9 Surface temperature rise plot in human eye as vitreous humour only tissue exposed to 2450 MHz-2600 MHz with side antennas at 3 cm.
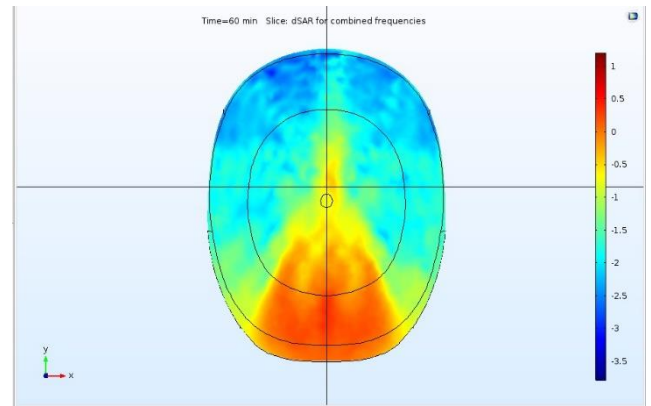
Figure 11 dSAR values on x-y plane with z=2.5 cm by 2450 MHz-2600 MHz with central antennas at 5 cm distance.

There is a verified relation between attention and blinking rate [16, 17]. During periods of increased cognitive load and focus on objects in the environment, the blinking rate decreases [16, 18]. Another study found decreased blinking rate during video terminal usage [19]. A VR environment not only increases the focus on objects, but also maximizes the cognitive load on the occipital and frontal lobes [20]. Nonetheless, if emotional stress is also involved, the blinking frequency has a strong correlation with the stress level [20]. Recalling our thermal isolation assumptions, the blinking would have marginal effects in a saturated vapor pressure environment. With the extra effects of decreasing blinking rates [16-20], it is quite a fair approximation, since the

Niyazi ULUAYDIN, Selim ŞEKER

Thermal Effect Estimation of Smartphone Virtual Reality Headsets on Human Eye by Finite Element Metho...

vapor pressure saturation may be achieved earlier in real world conditions than in simulations.

On the retinal part, retinal temperature increase is safe at 0.25°C at most by former retinal prosthesis research [21]. Certain retinal side effects such as retinal whitening, oedema, and fundus lesions can be observed with temperature rise over this value up to 2°C. And 2°C can be taken as a damage threshold level from cadaver and FEM studies [21]. In our first set of simulations, the highest corneal temperature increase was 0.35°C at a distance of 5 cm from face with 2450-2600 MHz pair (Figure 6). The highest temperature increase was rather on the nose (Figure 5).

Side antenna thermal effects were much more subtle. This time, both figures were almost doubled at the distance of 3 cm from face with 2450-2600 MHz (Figure 7,8). The corneal temperature increase reaches a total of 3.41°C, whereas retinal increase is at 0.12°C. This could be more disturbing for a child since their eye size is bigger compared to his/her cranium [22]. Another interesting observation in the side antennas' scenario is that only one of the eyes has an observable effect (Figure 9,10). The highest accumulated heat effect always occurred with 2450-2600 MHz pair in both cases.

On the logarithmic SAR values, there is a certain penetration into the center of the head, where endocrine glands may be affected (Figure 11). Athermal EM effects are statistically observable in pituitary glands [23,24]. At this level, one can presume similar effects on hypothalamus-thalamus and pineal glands, since they have similar tissue properties [25,26]. These endocrine glands have a vital effect on the hypothalamic–pituitary–adrenal (HPA) axis response and the circadian cycle (CC) of the body, respectively.

4. CONCLUSIONS

Our simulation results do not impose any immediate thermal biological effects; nonetheless, it may be possible to observe disturbing effects like dry eye syndrome with utilization of applications triggering high attention and high stress on SP VR headset.

The utilization of SP VR headsets for children may also raise concerns. Children up to age of 7 have bigger eyes relative to their head size and they are more prone to the effect of EM radiation. Our model provides the SAR penetration for the adult human head from SP VR headsets (Figure 11). Thus, one can assume further SAR penetration for a child head. It is possible to oversize the eye domain in our model, and one can simulate SP VR headset usage of children to an extent, too.

On the athermal effects, we have readily observed the effects on hypothalamus, thalamus, and pineal glands (Figure 11). There are similar SAR penetration values for the pituitary and parotid glands, too. For the first case, the antennas are positioned in an alignment with these three glands, and the nasal cavity may form a waveguide for the waves. In the latter case, there is no alignment but this time the distance is shorter, and there is not much of tissue to absorb the waves because of orbital and oral cavity. The first three are still more important on the homeostasis of humans, and thermal and athermal effects would be much more important because of HPA and CC. Such effects were already reported, too.

Our primary aim was to investigate the possible biological effects of SP VR headset usage with two concurrently active radio units' exposure. We have included all LTE bands below 3GHz such as 2300 and 2600 MHz. Our model has a novel approach over the classical SAR head phantom model with a special focus on a specific organ. Our model can further be customized for any other head organ in a similar way. Observed results of athermal effects on a specific part of the head confirmed by a group of studies can this way be linked back to a thermal threshold for that specific organ, such as pituitary glands. This new approach can totally change the classical thermal effect-only SAR exposure public safety standards. All EM exposure studies with confirmed observable athermal effects will be able to propose a more secure exposure standard with our SAR phantom head model modification approach.

Niyazi ULUAYDIN, Selim ŞEKER

Thermal Effect Estimation of Smartphone Virtual Reality Headsets on Human Eye by Finite Element Metho...

During the COVID-19 pandemic, VR/AR headset usage has further increased with distance working and home entertainment use. Therefore, we kindly recommend limiting the SP VR headset usage for children with the duration of 15 minutes at most based on our current saturation time measurements. It is equally important to provide air ventilation mechanism into the new SP VR headset designs.

Funding

The Declaration of Conflict of Interest/ Common Interest

No conflict of interest or common interest has been declared by the authors.

Authors' Contribution

The first author contributed 70%, the second author 30%.

The Declaration of Research and Publication Ethics

The authors of the paper declare that they comply with the scientific, ethical and quotation rules of SAUJS in all processes of the paper and that they do not make any falsification on the data collected. In addition, they declare that Sakarya University Journal of Science and its editorial board have no responsibility for any ethical violations that may be encountered, and that this study has not been evaluated in any academic publication environment other than Sakarya University Journal of Science.

REFERENCES

[1] Groupe Speciale Mobile Association https://www.gsma.com/, fetched at Feb 28, 2022.

[2] Statistica - Number of mobile augmented reality (AR) active users worldwide https://www.statista.com/statistics/1098630/global-mobile-augmented-reality-ar-users/, fetched at Feb 28, 2022.

[3] Groupe Speciale Mobile Association - A whole new ball game: when your living room becomes the sports stadium https://data.gsmaintelligence.com/research/research/research-2020/a-whole-new-ball-game-when-your-living-room-becomes-the-sports-stadium, Aug, 2020.

[4] Y. Diao, S.-W. Leung, Y. He, et al., "Detailed modeling of palpebral fissure and its influence on SAR and temperature rise in human eye under GHZ exposure," Bioelectromagnetics, vol. 37, no. 4, pp. 256-263, 2016.

[5] Y. K. E. Ng and E. H. Ooi, "FEM simulation of the eye structure with bioheat analysis," Computer methods and programs in biomedicine, vol. 82, no. 3, pp. 268-276, 2006.

[6] Comsol Multiphysics, www.comsol.com , COMSOL 4.3/4.3a FNL License No: 17073372.

[7] Comsol Absorbed Radiation (SAR) in Human Brain Model, https://www.comsol.com/model/absorbed-radiation-sar-in-the-human-brain-2190, fetched at July 28, 2021.

[8] Human Eye Model by Bobby Dyer, https://grabcad.com/library/human-eye-model/files , 2012.

[9] FCC Specific Absorption Rate for Cellular Phones https://www.fcc.gov/general/specific-absorption-rate-sar-cellular-telephones, fetched at July 28, 2021.

[10] G. Schmid, G. Neubauer, and P. R. Mazal, "Dielectric properties of human brain tissue measured less than 10 h postmortem at frequencies from 800 to 2450 MHz,"

Niyazi ULUAYDIN, Selim ŞEKER

Thermal Effect Estimation of Smartphone Virtual Reality Headsets on Human Eye by Finite Element Metho...

Bioelectromagnetics, vol. 24, no. 6, pp. 423-430, 2003.

[11] Levoy, M.: MRI data originally from Univ. of North Carolina (downloaded from the Stanford volume data archive at http://graphics.stanford.edu/data/voldata/ fetched at July 28, 2021).

[12] FCC Body Tissue Dielectric Properties https://www.fcc.gov/general/body-tissue-dielectric-parameters , fetched at July 28, 2021.

[13] E. H. Ooi, W.-T. Ang, and E. Y. K. Ng, "Bioheat transfer in the human eye: a boundary element approach," Engineering Analysis with Boundary Elements, vol. 31, no. 6, pp. 494-500, 2007.

[14] A. Karampatzakis and T. Samaras, "Numerical modeling of heat and mass transfer in the human eye under millimeter wave exposure," Bioelectromagnetics, vol. 34, no. 4, pp. 291-299, 2013.

[15] C. Li, Q. Chen, Y. Xie, and T. Wu, "Dosimetric study on eye's exposure to wide band radio frequency electromagnetic fields: Variability by the ocular axial length," Bioelectromagnetics, vol. 35, no. 5, pp. 324-336, 2014.

[16] T. Sakai, R. Yoshida, H. Tamaki, et al. "Electrodermal activity based study on the relationship between visual attention and eye blink," IEEE 9th International Conference In Sensing Technology (ICST), pp. 596-599, 2015.

[17] R. Yoshida, T. Sakai, Y. Ishi, et al. "Electrodermal activity-based feasibility study on the relationship between attention and blinking," International Journal on Smart Sensing & Intelligent Systems, vol. 9, no. 1, 2016.

[18] H. Ledger, "The effect cognitive load has on eye blinking," The Plymouth Student Scientist, vol. 6, no. 1, pp. 206-223, 2013.

[19] T. Schlote, G. Kadner, and N. Freudenthaler, "Marked reduction and distinct patterns of eye blinking in patients with moderately dry eyes during video display terminal use," Graefe's archive for clinical and experimental ophthalmology, vol. 242, no. 4, pp. 306-312, 2004.

[20] M. Haak, S. Bos, S.,Panic, and L. J. M. Rothkrantz, "Detecting stress using eye blinks and brain activity from EEG signals," Proceeding of the 1st driver car interaction and interface, pp. 35-60, 2009.

[21] N. L. Opie, A. N. Burkitt, H. Meffin, and D. B. Grayden, "Heating of the eye by a retinal prosthesis: modeling, cadaver and in vivo study," IEEE Transactions on Biomedical Engineering, vol. 59, no. 2, pp. 339-345, 2012.

[22] O. P. Gandhi, "Yes the children are more exposed to radiofrequency energy from mobile telephones than adults," IEEE Access, vol. 3, pp. 985-988, 2015.

[23] K. M. Abu Khadra, A. M. Khalil, M. Abu Samak, and A. Aljaberi, "Evaluation of selected biochemical parameters in the saliva of young males using mobile phones," Electromagnetic biology and medicine, vol. 34, no. 1, pp. 72-76, 2015.

[24] F. Söderqvist, M. Carlberg, and L. Hardell, "Biomarkers in volunteers exposed to mobile phone radiation," Toxicology letters, vol. 235, no. 2, pp. 140-146, 2015.

[25] S. A. Geronikolou A. Chamakou, A. Mantzou A., et al. "Frequent cellular phone use modifies hypothalamic–pituitary–adrenal axis response to a cellular phone call after mental stress in healthy children and adolescents: A pilot study," Science of the Total Environment, vol. 536, pp. 182-188, 2015.

[26] Z. Sienkiewicz, C. Calderón, K. A. Broom, D. Addison, et al. "Are Exposures to Multiple Frequencies the Key to Future

Radiofrequency Research?," Frontiers in public health, vol. 5, 2017.

Radiofrequency Research?," Frontiers in public health, vol. 5, 2017.